Dielectric Spectroscopy in the $\alpha\beta$ Splitting Region of Glass Transition in Poly(ethyl methacrylate) and Poly(*n*-butyl methacrylate): Different Evaluation Methods and Experimental Conditions

K. Schröter, R. Unger, S. Reissig, F. Garwe, S. Kahle, M. Beiner, and E. Donth*

Fachbereich Physik, Universität Halle, 06099 Halle (Saale), Germany

Received September 9, 1997; Revised Manuscript Received July 31, 1998

ABSTRACT: Stability of the dielectric parameters in the $\alpha\beta$ splitting region against methodical variations is demonstrated. The Williams product ansatz for correlation functions and an additive ansatz for dielectric functions are compared for poly(ethyl methacrylate). Both evaluation methods give a diminishing α intensity with increasing temperature, and a separate trace for the α relaxation different from both the secondary β relaxation below and the high-temperature *a* process above the crossover. Furthermore, measurements on different poly(*n*-butyl methacrylate) samples and evaluation results of different experimentalists are compared. The intensity onset of the cooperative α relaxation, starting from zero at a characteristic temperature T_{on} in the crossover region, and the parallel course of α and β relaxations below T_{on}, separated by about one frequency decade in an Arrhenius diagram, remain stable against measurement and evaluation variations.

A. Introduction

The dynamic glass transition (main transition or, conventionally, α relaxation) in low-molecular-weight glass formers, network glasses, and amorphous polymeric materials is usually accompanied by different secondary relaxations (β, γ relaxations and so on).[1,2] Whereas the glass transition at low temperatures is assumed to be caused by the cooperative motion of many particles, the secondary relaxations are of more localized molecular origin (for instance, Johari−Goldstein or β process).[3,4] This β process is distinct from the β_{fast} relaxation process in the picosecond time scale as described by the mode-coupling theory,[5] and distinct from the scattering effects at the boson peak.[6]

The temperature dependence of characteristic relaxation times $\tau = 1/\omega_{max}$ for the different processes can be visualized in an Arrhenius or activation diagram (log τ as a function of $1/T$, ω_{max} is the frequency of the maximum dynamic loss susceptibility, $\epsilon''(\omega)$ here). The main transition is characterized by a curved trace, in particular for fragile glass formers,[7] whereas the traces of the secondary relaxations usually are straight lines.

With increasing temperature and frequency the main transition and the β trace will usually approach each other.[1] This crossover region,[8] called the $\alpha\beta$ splitting region here, is of great importance for understanding the development of the glass transition below the crossover and the relation between both relaxation processes. To distinguish the qualitatively different relaxation processes of the main transition above and below the crossover we call the low-temperature part α and the high-temperature part *a*.[9]

The details of the $\alpha\beta$ splitting region were investigated in poly(*n*-alkyl methacrylate)s by means of broadband dielectric spectroscopy.[10] Supposing additivity of the α and β compliances, an intensity onset of the cooperative α process, starting from zero at a characteristic onset temperature T_{on}, was observed in all examples. For poly(*n*-butyl methacrylate) the traces of the developing α relaxation and the β relaxation are parallel in the crossover region, separated by about one frequency decade.

Similar results for the splitting region, especially the rapidly increasing intensity of the α process with decreasing temperature near the α onset, were also observed for polybutadiene[11] and epoxy resins[12,13] and for an organic glass-forming van der Waals liquid.[14]

The aim of this paper is to demonstrate the stability of these dielectric results. In section C two evaluation methods (Williams and additive ansatz) are compared for poly(ethyl methacrylate) (PEMA). In section D results from a broad variation of analysis methods, polymer samples, or measurement equipment are discussed for poly(*n*-butyl methacrylate) (PnBMA). Both polymers show the splitting region in a frequency range where high-precision dielectric data are available. This paper is not intended to discuss physical details behind the splitting scenario.[15]

B. Experimental Section

1. Materials. The characterization of the samples is listed in Table 1. The molecular weights were estimated by size exclusion chromatography. The glass transition temperature is defined by an equal-area construction of the specific heat in a heating run with 10 K/min following a cooling run with 10 K/min in a Perkin-Elmer DSC 7.

The poly(ethyl methacrylate) sample as well as the first poly(*n*-butyl methacrylate) sample (PnBMA1) listed in Table 1 were purchased from Polyscience. This PnBMA material was repeatedly measured over a time interval of 4 years. Results for one experimental series were published previously.[10]

Three further samples (PnBMA2, 3, and 4) were synthesized by Drs. S. Höring and S. Zeeb (University of Halle, Department of Chemistry). The first two have a broad molecular weight distribution, the last one is nearly monodisperse.

All samples were dried under vacuum to remove water, solvent, and residual monomer and then pressed between the electrodes for the dielectric measurements. Before investigation, all samples were annealed to yield a well-defined equilibrium. The preparation temperature never exceeded 130 °C to avoid thermal decomposition.

* E-mail: donth@physik.uni-halle.de.

10.1021/ma9713318 CCC: $15.00
Published on Web 11/14/1998

Table 1. Characterization of the Samples

sample	$10^{-3}\ M_w$	M_w/M_n	T_g °C
PEMA	154	1.9	74
PnBMA1	330	2.35	24
PnBMA2	1100	2.12	31
PnBMA3	560	1.6	31
PnBMA4	33.8	1.09	26

2. Dielectric Relaxation Measurements. The dielectric function $\epsilon^*(\omega) = \epsilon'(\omega) - i\epsilon''(\omega)$ was investigated by means of Novocontrol BDS 4000 instruments (Halle and Mainz) based on a Schlumberger frequency response analyzer FRA 1260 in a frequency range from $2\pi \times 10^{-2}$ to $2\pi \times 10^{7}$ rad s^{-1}. The depolarization current in the time domain was measured by Dr. Schönhals (Berlin) to enlarge the effective frequency interval down to $2\pi \times 10^{-4}$ rad s^{-1} for the PnBMA1 sample.[10] The $\tau \rightarrow \omega$ conversion used was described in ref 16.

C. Comparison of Williams Ansatz and Additive Ansatz for Poly(ethyl methacrylate)

1. Additive Compliances. In the case of strong overlap of two processes different approaches to the analysis of relaxation functions are possible. They are presently debated in the literature.[17] One possibility is a superposition ansatz of dielectric compliances $\epsilon^*(\omega)$ for α and β,[10] relying on thermodynamic arguments,[18] and a conductivity term $\epsilon''_\sigma \sim 1/\omega$,

$$\epsilon^*(\omega) = \epsilon^*_\alpha(\omega) + \epsilon^*_\beta(\omega) + \epsilon''_\sigma(\omega) \tag{1}$$

The only presupposition made for both relaxation processes is that each shape can be represented by an individual Havriliak−Negami (HN) function[19]

$$\epsilon^*(\omega) - \epsilon_\infty = \frac{\Delta\epsilon}{\left(1 + \left(i\frac{\omega}{\omega_0}\right)^b\right)^g} \tag{2}$$

This is a solid experimental fact[20] outside the splitting region (with no overlap).

In the HN function of eq 2, $\Delta\epsilon$ is the relaxation strength and ϵ_∞ is the real permittivity for high frequencies outside the dispersion zone. The loss-peak maximum frequency, ω_{max}, and the characteristic frequency, ω_0, are related by

$$\frac{\omega_{max}}{\omega_0} = \left(\frac{\sin\frac{\pi}{2}b}{\tan\frac{\pi b}{2(g+1)}} - \cos\frac{\pi}{2}b\right)^{-1/b} \tag{3}$$

The flexibility of the HN function is caused by two shape parameters b and g, which adjust independently the slopes of the log ϵ'' vs log ω curve below and above the loss-peak maximum frequency. Known peculiarities of the dielectric α process outside the peak region, like the "Nagel wing" in the high-frequency flank of the ϵ'' maximum,[21] cannot be represented by the HN function. Our measurement and fit range, however, is more centered on the peak regions. Furthermore, the Nagel wing is probably weak in the αβ splitting region and heavily masked by the strong β relaxation here.

Another unbiased method to separate different processes from a composite curve would be the determination of a continuous relaxation time spectrum $g(\tau)$[22−24]

$$\epsilon''(\omega) = \int_0^\infty g(\tau)\frac{\omega\tau}{1 + (\omega\tau)^2}\,d\tau \tag{4}$$

As long as separate peaks or shoulders are resolved, they are associated with different mechanisms. But the determination of a spectrum usually corresponds to the estimation of a large number of fit parameters. To get reliable results from many data points, highly sophisticated mathematical regularization methods are applied.[25] The regularization parameter effectively reduces the number of fit parameters by damping the "roughness" of the resulting spectrum. Relaxation-time spectra were estimated by the NLREG regularization program[25] using the compliance formalism similar to[24] for synthetic frequency-domain data corresponding to typical intensity and relaxation time parameters in the crossover region of PEMA. The regularization program was not able to resolve the strong overlap of both relaxation processes if they were separated by one frequency decade.

2. Williams Correlation Function. An alternative approach was suggested by Williams[26] for the time domain. It is based on an additive formula, combined with a product ansatz from underlying α and β processes. The product was interpreted by statistical independence.

$$\varphi(t) = f_\alpha\varphi_\alpha(t) + (1 - f_\alpha)\varphi_\alpha(t)\varphi_\beta(t) \tag{5}$$

The relaxation functions $\varphi_i(t)$, i = α or β, are defined via dielectric compliance (see below). Both relaxation functions, $\varphi_\alpha(t)$ and $\varphi_\beta(t)$, correspond, via the fluctuation dissipation theorem FDT, to autocorrelation functions of polarization fluctuations, with the property $|\varphi_i(t)| \le \varphi_i(0) = 1$, $t \ge 0$. The relative strength factor for the α process, f_α, $0 \le f_\alpha \le 1$, is considered as the relative fraction of the polarization relaxed *only* by the α relaxation, i.e., with no β assistance.

For practical reasons, a presupposition for the shape of the individual relaxation functions is also necessary. Usually, the α relaxation is described by a stretched exponential or Kohlrausch (KWW) function[27]

$$\varphi_\alpha(t) = \exp\left(-\left(\frac{t}{\tau_{KWW}}\right)^{\beta_{KWW}}\right) \tag{6}$$

with a characteristic exponent, β_{KWW}, $0 < \beta_{KWW} \le 1$, and a relaxation time, τ_{KWW}. In this case the loss-peak maximum frequency, ω_{max}, and the relaxation time, τ_{KWW}, are related by[28,29]

$$\log_{10}(\omega_{max}\tau_{KWW}) = -0.263(1 - \beta) \tag{7}$$

The secondary β relaxation can often be described by a symmetrical function, for instance a Cole−Cole function.[30]

3. Data Evaluation. The additive and the Williams approaches are compared for poly(ethyl methacrylate). PEMA is better suited than PnBMA for this purpose because of the wider frequency separation between α and β relaxation at low temperatures. This is necessary for a separate determination and the reasonable extrapolation of the individual β relaxation into the crossover region in the case of the Williams ansatz. The identity of the α and β mechanisms in the crossover region is defined by extrapolations from low-tempera-

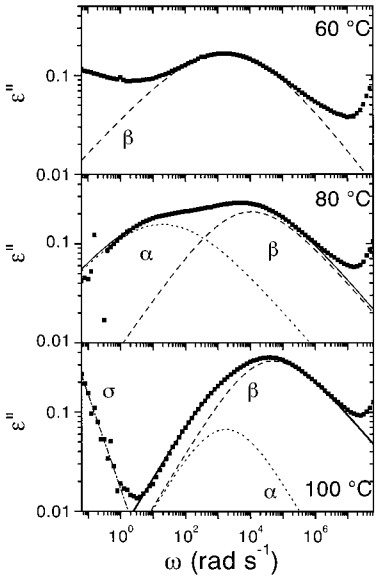

Figure 1. Frequency dependence of the imaginary part $\epsilon''(\omega)$ of the dielectric function for PEMA at selected temperatures of 60, 80, and 100 °C. For the 60 °C isotherm a fit to the β relaxation process with a symmetrical Havriliak–Negami function is shown. For the other temperatures the result of a fit with an additive ansatz of α and β relaxation is shown.

ture behavior, where α and β are well separated and, therefore, well defined.[11]

Figure 1 shows the experimental imaginary part of the dielectric function of PEMA for selected temperatures. For low temperatures, α and β relaxation are well separated, but they increasingly overlap with increasing temperature to form finally a single high-temperature relaxation. The upturn in the imaginary part at low and high frequencies corresponds to the influence of sample conductivity and a resonance artifact of the measuring device, respectively.

First, the data were analyzed according to the additive approach[10] in the frequency domain. Two Havriliak–Negami functions were used for α and β relaxation. The intensity, frequency position, and shape parameters were left free in the fit procedure. The results for the three isotherms are included in Figure 1.

To perform the analysis with the Williams ansatz (eq 5) the dielectric compliance $\epsilon^*(\omega)$, measured in the frequency domain, has to be transformed to the time domain. A direct Fourier transform of the data is not recommended because the limited bandwidth of the measurements causes serious truncation errors. In a first step we used the NLREG regularization program mentioned above to estimate relaxation time spectra g (ln τ) from the data. These spectra only serve to represent the data and to estimate the time functions $\epsilon(t)$ by integration. The conductivity term is separated from the spectra as an extra parameter by the regularization program. The high-frequency resonance of the dielectric setup was truncated in the spectra at the minimum between relaxation processes and resonance.

In a second step the dielectric function $\epsilon(t)$ in the time domain can be calculated by

$$\epsilon(t) = \epsilon_\infty + \int_{-\infty}^{+\infty} g(\ln \tau)\left(1 - \exp\left(-\frac{t}{\tau}\right)\right) \mathrm{d}(\ln \tau) \quad (8)$$

Figure 2 shows the result for the same temperatures as in Figure 1. The composite relaxation shows a decreasing strength with increasing temperature. In

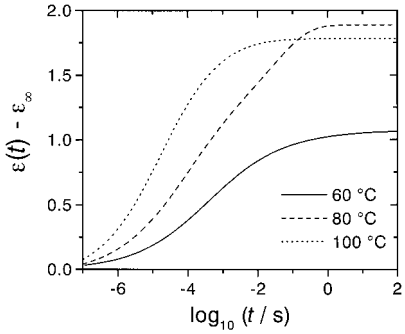

Figure 2. Dielectric relaxation function $\epsilon(t)$ for the same temperatures as in Figure 1.

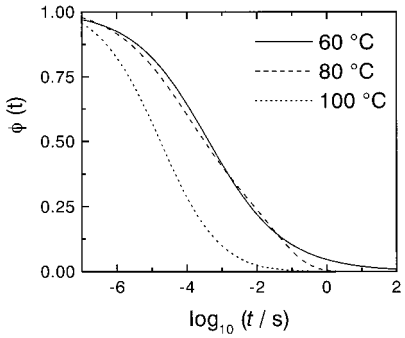

Figure 3. Normalized relaxation function $\varphi(t)$ for the same temperatures as in Figure 1.

the 60 °C isotherm only the β relaxation process (cf. Figure 1) is visible. This explains the lower value of $\epsilon(t)$ for long times.

In a third step, the desired relaxation function $\varphi(t)$ was calculated from $\epsilon(t)$ by normalization.[31]

$$1 - \varphi(t) = \frac{\epsilon(t) - \epsilon_\infty}{\epsilon(\infty) - \epsilon_\infty} \quad (9)$$

The value $\epsilon(\infty)$ was estimated from the sum over the whole spectrum

$$\epsilon(\infty) - \epsilon_\infty = \int_{-\infty}^{+\infty} g(\ln \tau)\, \mathrm{d}(\ln \tau) \quad (10)$$

and contains, of course, only contributions from the experimental frequency range.

Figure 3 shows the relaxation functions $\varphi(t)$ for the same temperatures as in Figure 1. The different relaxation processes are only visible as parts of different slopes. In the Williams analysis these curves were then subjected to a fit procedure utilizing a Levenberg–Marquard algorithm.[32] For low temperatures the individual β relaxation peaks were fitted with a Havriliak–Negami function, eq 2. A value of almost $g = 1$ was obtained, which corresponds to a Cole–Cole function, as expected for a secondary relaxation. Figure 1 shows such a fit as an example for the 60 °C isotherm. The increase with temperature of the other shape parameter b_{cc} was linearly extrapolated to the crossover region in analogy to ref 11 (Figure 4). The α relaxation parameter τ_{KWW} and intensity f_α were free fit parameters. Additionally, also the KWW exponent β_{KWW} was left free here.

To utilize eq 5 in the fit procedure, the relaxation function $\varphi_\beta(t)$ in the time domain has to be estimated from the Cole–Cole function in the frequency domain. This was done numerically. For frequencies outside the

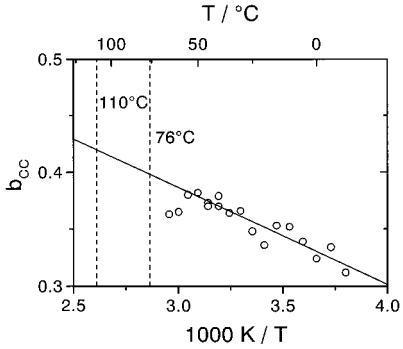

Figure 4. Temperature dependence of the Cole−Cole parameter b_{cc} for the β relaxation of PEMA.

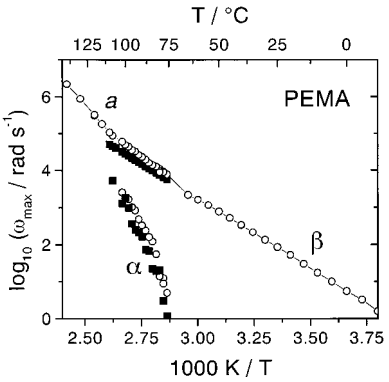

Figure 5. Frequency of the loss maxima, ω_{max} for α and β relaxations as a function of reciprocal temperature for PEMA. The solid symbols are for the Williams and the open symbols for the additive ansatz.

peak region asymptotic series expansions were used. In a frequency interval of about three decades around the peak frequency the relaxation function was calculated by numerical integration of the spectrum

$$\varphi_\beta(t) = \int_{-\infty}^{+\infty} \exp\left(-\frac{t}{\tau}\right) g_{cc}(\ln \tau)\, d(\ln \tau) \qquad (11)$$

with

$$g_{cc}(\ln \tau) = \frac{1}{2\pi} \frac{\sin[(1 - b_{cc})\pi]}{\cosh[b_{cc} \ln(1/\tau\omega_0)] - \cos[(1 - b_{cc})\pi]} \qquad (12)$$

The Cole−Cole parameter b_{cc} was taken from Figure 4.

4. Comparison of Results. Figure 5 shows the temperature dependence of the peak frequencies for α and β relaxation processes from both evaluation approaches. The peak frequencies for the imaginary parts were estimated from the fit results as described. Both approaches give comparable traces for the relaxation processes.

Figure 6 shows the temperature dependence of the α relaxation intensity, given as $\Delta\epsilon_\alpha$ for the additive ansatz and as f_α for the Williams ansatz. Both methods result in a diminishing α intensity for increasing temperature. A linear extrapolation to zero intensity gives an onset temperature of $T_{on} = 110$ °C ± 10 K for both methods.

Above the onset temperature the Williams ansatz formally permits Arbe et al. to maintain the α process as $\varphi_\alpha(t)$ in the product term of eq 5.[11] In the case of PEMA the fit routine gives no stable results there. The results do not seem to justify the idea that the high-

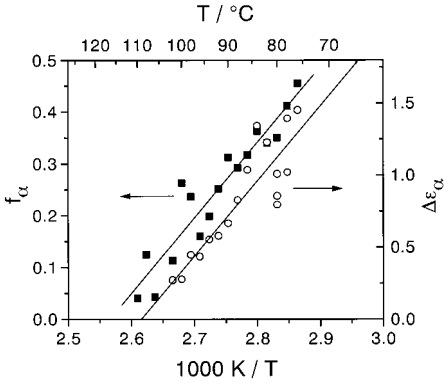

Figure 6. Intensity of dielectric α relaxation process for PEMA as a function of reciprocal temperature. For the Williams ansatz the value f_α (■) and for the additive ansatz $\Delta\epsilon_\alpha$ (○) is given, respectively. The scales are chosen so that equal slopes are obtained.

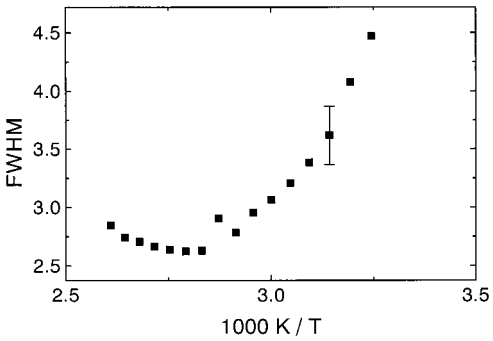

Figure 7. Total logarithmic frequency width at half-maximum (fwhm) of the imaginary part $\epsilon''(\omega)$ as a function of reciprocal temperature for the PnBMA3 sample. The error bar indicates a typical error.

temperature *a* process can be considered as a continuation of the low-temperature α and β processes.

D. Influence of Experimental Parameters for Poly(*n*-butyl methacrylate)

In addition to our first investigation on a polydisperse, high-molecular weight PnBMA,[10] a systematic study of possible influences of experimental parameters or evaluation procedures was accomplished. Measurements on different samples and equipments (see Experimental Section) were compared, the same sample was repeatedly measured, and the data were independently evaluated by different experimentalists and with two different fit routines. Because of the complicated structure of the fit deviation surface, with many local minima in the parameter space, the determination of the global deviation minimum by nonlinear regression is difficult and may possibly depend on the strategy of the fitting routine or the experimentalist. Uncertainties arise also from the restricted data sets and random experimental errors.

In a first step of data evaluation, the total logarithmic frequency width at half-maximum (fwhm) of the imaginary part $\epsilon''(\omega)$ was calculated directly from the measured isotherms $\epsilon''(\omega)$ without using any fit routine. As shown in Figure 7 as an example for PnBMA3, a strong increase of fwhm below a certain temperature (in this case approximately below 70 °C) indicates a fundamental change in the relaxation mechanism.

The details of this relaxation mechanism were further analyzed using the additive fit procedure. In all cases

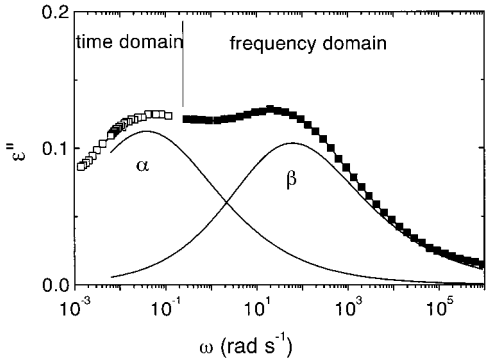

Figure 8. Frequency dependence of the imaginary part $\epsilon''(\omega)$ of the dielectric function for the PnBMA1 sample at a temperature of 24 °C. The curves are the two Havriliak−Negami fit functions for α and β.

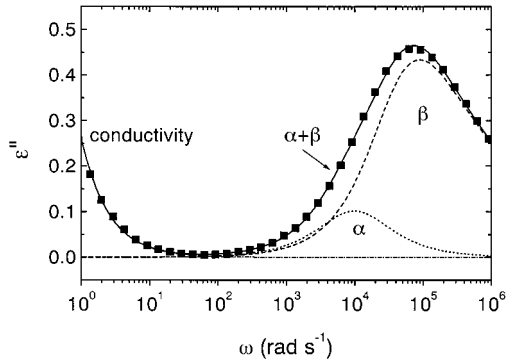

Figure 9. Frequency dependence of the imaginary part $\epsilon''(\omega)$ of the dielectric function for the PnBMA1 sample at a temperature of 80 °C. The two Havriliak−Negami fit functions for the α and β process are shown, too.

the measured real and imaginary parts of the dielectric function were simultaneously fitted to one or a sum of two HN functions (additive ansatz) and a conductivity term $\epsilon'' \sim 1/\omega$. As shown in the previous paragraph, the results do not heavily depend on the evaluation method.

The fit was performed by two different computer programs. Program 1[33] uses a Gaussian least-squares method. Program 2 was developed using the Levenberg−Marquard algorithm.[32] The data evaluation started in all cases at isotherms with well-separated α and β processes at low temperatures. The estimated parameters were used as starting values for the fit of the next isotherm. Differences in the results arise from the subjective cut of measurement points at the edges of the dispersion zones to avoid, for instance, the influence of the conductivity flank or a high-frequency (HF) resonance of the apparatus on the fit results. This point will be discussed below. All relaxation parameters are considered to be free.

The success of the fit procedures is strongly influenced by the position of the dispersion zones within the frequency window of the experiments, their mutual positions and intensities, the superposition of different processes (ionic conductivity and Maxwell−Wagners-Sillers (space charge) effect;[34] see Figure 9, below), and the HF resonance of the device.

The first problem of the limited frequency range is shown in Figure 8. For 24 °C both the α and β process maxima are well separated. This separation, however, is explicitly evident only after the addition of time-domain values to the frequency-domain data. For this

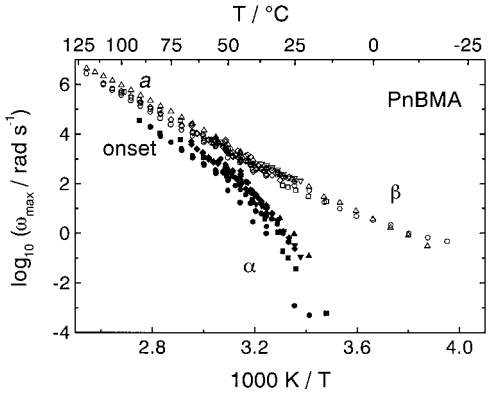

Figure 10. Frequency of the loss maxima, ω_{max}, of the Havriliak−Negami fit functions as a function of reciprocal temperature for all experiments. The solid and open symbols are for the α and β relaxations, respectively.

case, the determination of both loss peak frequencies, ω_{max}, for the Arrhenius diagram is possible without ambiguity. In the case of frequency-domain investigations alone, the low-frequency flank of the α process leaves the available frequency window. Since the intensity of this process corresponds to the ϵ'' vs log ω curve area, the precise intensity determination would require additional low-frequency measurements or must be based on an extrapolation of the low-frequency peak flank (the HN parameter *b*).

The problems of dispersion-zone positions and the influence of a conductivity process are presented in Figure 9. At a temperature of 80 °C (see Figure 2 of ref 10) both processes are well situated in the experimental frequency window. But they are only slightly separated on the frequency scale, and the intensity ratio has changed in comparison to $T = 24$ °C. The intensity of the low-frequency α process is diminished, and it is difficult to resolve it from the β process flank. Furthermore, this frequency range is also influenced by the conductivity flank at lower frequencies. Therefore, the α process intensity and the α log ω_{max} position become more and more uncertain.

The investigation of samples differently prepared leads to slight deviations of dispersion intensities and positions. As stated earlier,[10] the details in the splitting region (also considering the influence of conductivity flank) depend rather sensitively on unknown molecular and synthesis details, which may change with time or handling. These deviations, however, do not alter the splitting scenario (see below). An important reason for differences in the height of the dielectric loss maximum are geometrical differences of different experimental runs. This results mainly from sample thickness inaccuracies. Spacers fixing the electrode distance were not used to avoid conductivity effects.

Furthermore, the dielectric function is influenced by the intrinsic temperature-dependent ionic conductivity. This effect differs from sample to sample. The other electrical problems such as sample cell resonance effects at frequencies above $2\pi \times 10^6$ rad s^{-1} due to feed lines and a measurement-range switching effect at about $2\pi \times 10^4$ rad s^{-1}, yielding a small shift in ϵ'', play only a minor role in our case: The overlap region of the high-frequency flank of the α dispersion zone and the low-frequency flank of the β zone is not influenced.

Figure 10 compares the temperature dependence of ω_{max} for all experiments accomplished by the different experimentalists on the four different PnBMA samples.

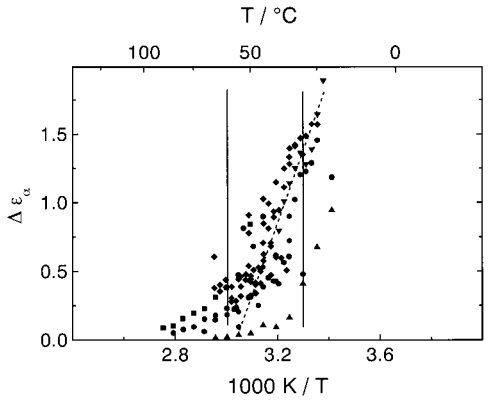

Figure 11. $\Delta\epsilon_\alpha$ intensity of the dielectric α relaxation process for all evaluations as a function of reciprocal temperature. The vertical lines indicate the region of the more reliable results between approximately 30 and 60 °C. The dashed line gives the general trend as expected from a theoretical consideration.[15]

All traces group to two dispersion zones α (lower part of main transition) and *βa* (continuous trace for the *β* and the high-temperature *a* relaxation). The differences between the separate investigations do not break the topological structure of the relaxation map, namely the existence of two separated traces. We find an onset of the α relaxation below the continuous trace for the *β* and *a* relaxations, and a parallel course of *a* and α in the crossover region. The onset of α relaxation corresponds to the strong fwhm increase in Figure 7.

The temperature dependence of the $\Delta\epsilon$ intensities for the different processes is important for our physical interpretation,[15] even if their absolute values are influenced by the sample thickness error mentioned above. The main problem arises from the fit with two HN functions of strongly different intensity in the crossover region, as discussed in connection with Figure 9.

Figure 11 shows the $\Delta\epsilon_\alpha$ temperature dependence for the different measurements and evaluations. The vertical lines indicate a temperature region of the more reliable results. As explained in the discussion for Figures 8 and 9, the intensities become uncertain at low and high temperatures. As mentioned above, the low-temperature deviations are partly due to missing low-frequency measurements.

Different intensities at the same temperature for the same investigation result from repeated fits with slightly different starting parameters. All evaluations clearly show that the α intensity at high temperatures steeply decreases. A considerable scatter can be observed mainly at higher temperatures in the region of a high intensity ratio between *β* and α. Nevertheless, the overall trend of a diminishing α relaxation intensity with increasing temperature (α intensity onset $\Delta\epsilon_\alpha = 0$ at an extrapolated onset temperature) is preserved. Suppressing a possible 10% tail in $\Delta\epsilon_\alpha$ at higher temperatures, a linear $\Delta\epsilon_\alpha - T$ (or $\Delta\epsilon_\alpha - 1/T$) extrapolation to an onset temperature $T_{on} \approx 50$ °C with $\Delta\epsilon_\alpha \rightarrow 0$ seems reasonable.

Possibly, the data are also influenced by changes in molecular details with time or preparation and by differences between different samples in this sensitive splitting region. This needs further investigation.

A dashed straight line in Figure 11 indicates the general trend physically explained by a theoretical model of the cooperativity onset.[15] Heat capacity spectroscopy is only sensitive to the cooperative α relaxation. Corresponding heat capacity and dielectric measurements on statistical copolymers of *n*-butyl methacrylate with styrene support the onset concept.[9] A DSC study of the homologous series of the *n*-alkyl methacrylates also indicates a diminishing α intensity ΔC_p.[35]

E. Conclusions

The dielectric relaxation in the αβ splitting region of poly(ethyl methacrylate) and poly(*n*-butyl methacrylate) was investigated. For poly(ethyl methacrylate) the Williams and a simple additive ansatz for the dielectric functions are compared for the same data set. For poly(*n*-butyl methacrylate) measurements on different samples and evaluation results of different experimentalists are compared. In this case the dielectric function was fitted by one or a sum of two HN functions to separate the α and *β* relaxation processes (additive ansatz).

For both substances, irrespective of evaluation method or individual sample, the intensity of the α relaxation diminishes with increasing temperature. We find always a separate onset of the α relaxation below the continuous trace for the local *β* and high-temperature *a* relaxation. The latter has distinctly different relaxation parameters than both the low-temperature α and the *β* relaxation.

Our comparison of evaluation methods and our results on different samples confirm the onset concept for the α relaxation. They show clear indications for a fundamental change of relaxation mechanism in the crossover region. This limits the applicability of extrapolation of low-temperature relaxation results to higher temperatures. It seems more appropriate "that the single loss process above 100 °C which emerges after the α and *β* processes have coalesced is a distinct and separate process", as Williams noticed for PEMA already in 1966.[36]

Acknowledgment. The authors are grateful to the Deutsche Forschungsgemeinschaft, the Fonds der Chemischen Industrie, and the Land Sachsen-Anhalt for financial support. We thank the Max-Planck Institute für Polymerforschung in Mainz for its experimental aid, Dr. Schönhals (Berlin) for the time-domain measurements, and Dr. Höring and Dr. Zeeb (Halle) for the synthesis of three samples.

References and Notes

(1) Williams, G. *Adv. Polym. Sci.* **1979**, *33*, 59.
(2) McCrum, N. G.; Read, B. E.; Williams, G. *Inelastic and Dielectric Effects in Polymeric Solids*; London: Wiley: 1967 (reprint: Dover, New York, 1991).
(3) Johari, G. P.; Goldstein, M. *J. Chem. Phys.* **1970**, *53*, 2372. Johari, G. P.; Goldstein, M. *J. Phys. Chem.* **1970**, *74*, 2034. Johari, G. P. *Ann. N. Y. Acad. Sci.* **1976**, *279*, 117.
(4) Cowie, J. M. G. *J. Macromol. Sci., Part B: Phys.* **1980**, *18*, 569.
(5) Götze, W.; Sjörgren, L. *Rep. Prog. Phys.* **1992**, *55*, 241.
(6) Buchenau, U. *Philos. Mag. B* **1992**, *65*, 303.
(7) Angell, C. A. In *Relaxations in Complex Systems;* Ngai, K. L., Wright, G. B., Eds.; Government Printing Office: Washington, DC, 1985; p 1.
(8) Sokolov, A. P. *Endeavour* **1997**, *21*, 109.
(9) Kahle, S.; Korus, J.; Hempel, E.; Unger, R.; Höring, S.; Schröter, K.; Donth, E. *Macromolecules* **1997**, *30*, 7214.
(10) Garwe, F.; Schönhals, A.; Lockwenz, H.; Beiner, M.; Schröter, K.; Donth, E. *Macromolecules* **1996**, *29*, 247.
(11) Arbe, A.; Richter, D.; Colmenero, J.; Farago, B. *Phys. Rev. E* **1996**, *54*, 3853.

(12) Casalini, R.; Fioretto, D.; Livi, A.; Lucchesi, M.; Rolla, P. A. *Phys. Rev. B* **1997**, *56*, 3016.
(13) Corezzi, S.; Capaccioli, S.; Gallone, G.; Livi, A.; Rolla, P. A. *J. Phys.: Condens. Matter* **1997**, *9*, 6199.
(14) Alvarez, F.; Hoffman, A.; Alegria, A.; Colmenero, J. *J. Chem. Phys.* **1996**, *105*, 432.
(15) Donth, E.; Kahle, S.; Korus, J.; Beiner, M. *J. Phys. I Fr.* **1997**, *7*, 581.
(16) Schönhals, A. *Acta Polym.* **1991**, *42*, 149.
(17) Donth, E.; Schröter, K.; Kahle, S. To be published. Reply: Arbe, A.; Richter, D.; Colmenero, J.; Farago, B. To be published.
(18) Donth, E. *J. Polym. Sci., Part B: Polym. Phys.* **1996**, *34*, 2881.
(19) Havriliak, S.; Negami, S. *J. Polym. Sci., Part C* **1966**, *14*, 99.
(20) Havriliak, S., Jr.; Havriliak, S. J. *J. Noncryst. Solids* **1994**, *172*, Part 1, 297.
(21) Dixon, P. K.; Wu, L.; Nagel, S. R.; Williams, B. D.; Carini, J. P. *Phys. Rev. Lett.* **1990**, *65*, 1108.
(22) Ferry, J. D.; Strella, S. *J. Colloid Sci.* **1958**, *13*, 459.
(23) Imanishi, Y.; Adachi, K.; Kotaka, T. *J. Chem. Phys.* **1988**, *89*, 7593.
(24) Schäfer, H.; Sternin, E.; Stannarius, R.; Arndt, M.; Kremer, F. *Phys. Rev. Lett.* **1996**, *76*, 2177.
(25) Honerkamp, J.; Weese, J. *Rheol. Acta* **1993**, *32*, 65.
(26) Williams, G.; Watts, D. C. In *NMR Basic Principles and Progress*; Diehl, P., Fluck, E., Kosfeld, R., Eds.; Berlin: Springer, 1971; Vol. 4, p 271.
(27) Kohlrausch, R. *Ann. Phys.* **1847**, *12*, 393.
(28) Williams, G.; Watts, D. C.; Dev, S. B.; North, A. M. *Trans. Faraday Soc.* **1971**, *67*, 1323.
(29) Lellinger, D., et al., unpublished work, 1994.
(30) Cole, K. S.; Cole, R. H. *J. Chem. Phys.* **1941**, *9*, 341.
(31) Williams, G. *Chem. Soc. Rev.* **1978**, *7*, 89.
(32) Press, W. H.; Flannery, B. P.; Teukolsky, S. A.; Vetterling, W. T. *Numerical Recipes in Pascal (Fortran, C). The Art of Scientific Computing*; Cambridge University Press: Cambridge, NY, 1992; p 574.
(33) Schlosser, E.; Schönhals, A. *Colloid Polym. Sci.* **1989**, *267*, 133.
(34) Maxwell, J. C. *Electricity and Magnetism*; Claredon: Oxford, U.K., 1892; Vol. 1, p 425. Wagner, K. W. *Arch. Elektrotech.* **1914**, *2*, 371. Sillars, R. W. *J. Inst. Elect. Eng.* **1937**, *80*, 378.
(35) Hempel, E.; Beiner, M.; Renner, T.; Donth, E. *Acta Polym.* **1996**, *47*, 525.
(36) Williams, G. *Trans. Faraday Soc.* **1966**, *62*, 2091.

MA9713318